J Fluoresc (2008) 18:203–217
DOI 10.1007/s10895-007-0264-3

ORIGINAL PAPER

Fluorescence Dynamics of Three UV-B Sunscreens

Rajagopal Krishnan · Thomas M. Nordlund

Received: 7 June 2007 / Accepted: 24 September 2007 / Published online: 26 October 2007

Abstract Polarity of the surrounding medium affects the excited states of UV-B sunscreens. Therefore understanding excited state processes in a mixed polarity model system similar to skin is essential. We report the excited state lifetimes, quantum yields, radiative and non-radiative rates of three sunscreens. Among the three UV-B sunscreens studied, octyl salicylate emits from a single excited state, while padimate O and octyl methoxy cinnamate show multiple states. The radiative rates of salicylate and cinnamate are approximately constant, while that of padimate O depends strongly on solvent. The non-radiative rates of all sunscreens vary with solvent polarity. Compared to salicylate and cinnamate, padimate O is complex to analyze because of its two emission peaks and one peak's strong dependence on the dielectric constant. High absorbance, broad absorption peak with small fluorescence quantum yield, and low radiative rate make octyl methoxy cinnamate a superior UV-B sunscreen ingredient. The complexity in excited-state analysis shows that the lifetimes of the sunscreens are critical parameters, in addition to absorbance and quantum yield. Fluorescence lifetime substantiates the use of polystyrene nanospheres as a model host to study the photo-physical properties of sunscreen in a heterogeneous environment.

Keywords Sunscreen · Excited states · Fluorescence · UV-B · Dynamics

R. Krishnan · T. M. Nordlund (✉)
Department of Physics, University of Alabama at Birmingham,
CH 310, 1530 3rd Avenue South,
Birmingham, AL 35294-1170, USA
e-mail: nordlund@uab.edu

Introduction

The effectiveness of organic sunscreens is primarily based on absorption wavelength and absorption coefficient. Absorption studies of sunscreens are often conducted in solvents forming good solutions that are easy to study with standard spectrophotometers [1–4]. The absorption of these molecules is found to be dependent on the polarity of the medium [5]. In general, low solvent polarity lowers the ground state energy of the hydrophobic molecule and moves the wavelength region of absorption farther to the UV by raising the excitation energy. However, more complex behavior is observed in some sunscreens, with red shifts in solvents of low polarity [5]. Using Raman spectroscopy it was found that effects of polarity of medium on the ground state of sunscreens like octyl salicylate, padimate O and octyl methoxy cinnamate are through charge transfer and hydrogen-bonding interactions [6]. The hydrogen bonds are formed intramolecularly or with solvent, accompanied by conformational changes.

Although absorption is the primary property used to decide whether a molecule can act as an effective sunscreen, after-absorption processes are equally important. Some important after-excitation parameters of sunscreen molecules are radiative, non-radiative and intersystem crossing rates. All these rates help determine the excited-state lifetimes. There can be other after-excitation processes, such as energy transfer and radical formation. These processes also depend on the de-excitation rates of the sunscreen. In addition to the processes themselves, particular after-excitation process dominant in a non-polar environment may be virtually absent in a polar environment. Hence, the medium in which the sunscreens are present plays a significant role in determining which photophysical parameters are important. Further, the after-excitation processes of sunscreens applied

to skin can have effects distant from the site of application [7]. The final location of sunscreen molecules such as octyl salicylate, octyl methoxy cinnamate, and padimate O applied to skin could be a cell surface, keratin layer, or aqueous cellular compartments in liposomes of stratum corneum. Though most penetration studies of sunscreen ingredients into skin show the outer layer (stratum corneum) to harbor most of the screening agents, the penetration through this layer into living cells depends on the agent or combination of agents, skin thickness, and the carriers used in the lotion [8].

Sunscreens are present in a heterogeneous environment (hydrophobic/hydrophilic and polar/non-polar environment of stratum corneum) in skin. Therefore, studies of sunscreens in neat solvent produce results of questionable relevance to those in skin. Therefore, it is necessary to understand the after-excitation processes of sunscreens in a skin-like system. A heterogeneous system like skin can be adequately simulated by the confinement of groups of sunscreen molecules to micron- or submicron-sized, low-dielectric structures, dispersed in a buffered, aqueous medium. The surface of these dispersed structures presents a hydrophobic environment to the sunscreens, while the system (micro-structures + sunscreens) remains in hydrophilic environment. Hence, the structures can act as an in vitro model for studying sunscreen molecules in a mixed dielectric microenvironment where one can observe the effects on electronic spectra. In previous work, we showed polystyrene nanosphere suspensions can be used as model system for a mixed-polarity environment. In that work, we studied the effects of solvents on the absorption and the steady state fluorescence of sunscreens and compared with the effects of polystyrene nanospheres [9]. Since the results suggested that the after-excitation processes are more sensitive to the polarity than is absorption, we used fluorescence spectroscopy to establish the polystyrene nanospheres as a model system in our subsequent work. In that study we compared the sunscreens emission in nanosphere, HaCat cell and skin environments [10]. In addition, we showed that the nanosphere system could be used to measure the effectiveness (absorbance) of sunscreen [11].

Due to the importance of the dielectric constant/polarity effect on sunscreen fluorescence, we now study the same sunscreens by time-resolved fluorescence to understand the mechanism of the observed fluorescence in steady state spectra. In this work we present excited state lifetimes, quantum yields, radiative and non-radiative rates of the UV-B sunscreen molecules in solvents. We observe a surprising result in padimate O and octyl methoxy cinnamate, the presence of a fast- and a slow-relaxing state, the latter producing most steady state emission. Comparing the lifetimes of sunscreen in toluene with those in the nanosphere system, we show that behavior of the sunscreens in the mixed polarity medium is dominated by the low polarity region.

Materials and methods

Spheres and sunscreens Size-classified 220 nm polystyrene spheres were obtained from Interfacial Dynamics Corporation (Tualatin, OR). Octyl salicylate (2-ethylhexyl salicylate) was obtained from BF Goodrich Performance Materials (Cleveland, OH) while octyl methoxycinnamate (2-ethylhexyl-4-methoxycinnamate) and padimate O (2-ethylhexyl 4-(dimethylamino)benzoate) came from Spectrum Quality Products Inc. (Gardena, CA).

Sunscreens in solvents Pure octyl salicylate, octyl methoxy cinnamate, and padimate O were diluted in organic solvents methanol, 1-propanol, toluene, or ethyl acetate, to give a concentration of 5 or 10 mM stock solution. These stock solutions were further diluted in the corresponding solvents to give final concentrations of 5 μM for octyl salicylate samples and 10 μM for octyl methoxy cinnamate and padimate O.

Sphere-sunscreen sample Concentrated suspensions of the spheres were diluted in 20 mM Tris-buffer (pH~7.3) containing 100 mM KCl and 0.1 mM EDTA. Concentrations of diluted 220 nm sphere suspensions for sphere-salicylate and sphere padimate O samples were 16 pM and 76 pM (0.0096 and 0.046 spheres/$(\mu m)^3$) respectively. Sphere-sunscreen suspensions were prepared by adding sunscreen stock solution to the diluted sphere suspension to give a final concentration of 5 μM octyl salicylate or 10 μM padimate O and vortex mixing for 30 s.

Instrumentation Absorption-scattering spectra were measured with a Jasco V-530 photodiode-based UV/VIS Spectrophotometer (JASCO Corporation, Tokyo, Japan) using 0.3 cm path length cuvettes. Fluorescence decays were measured with a microchannel plate photomultiplier from Hamamatsu (R3809U-50). This photomultiplier has a broad spectral response from 200 to 800 nm and fast response time (as short as 37 ps). A PicoQuant PCI-Board for Time-Correlated single photon counting operated by TimeHarp 200 software version 3.0 was used for photon counting. The excitation light source used for this measurement was a femtosecond Ti:sapphire laser (Coherent Mira 900). The high repetition rate (76 MHz) of the Ti:sapphire laser was lowered to 3.8 MHz (20-fold) using a pulse picker (Coherent 9200) to accommodate the timing capability of electronics system. The fundamental output wavelength of the laser was tuned to 875 nm and frequency tripled to 292 nm. Though most sunscreen excitation peaks are near 310 nm, the laser wavelength represented the best compromise, at the time, between wavelength and power. The lower laser power increased the timing jitter and broadened the system response function (measured FWHM) to about 350 ps. This broadening of the response function does not affect the fitted lifetimes

of the sunscreens because the shortest lifetime, 140 ps, can still be clearly resolved through system response convolution. The decay data from the TimeHarp 200 software were deconvoluted and analyzed by Globals fluorescence decay software (Laboratory for Fluorescence Dynamics, Department of Physics, University of Illinois, Urbana, IL). Global fluorescence decay software uses least-squares analysis to obtain the best fit with a particular exponential model. The parameter which defines the quality of the fit is χ_R^2 (residual χ^2), which is given by

$$\chi^2 = \sum_{k=1}^{n} \frac{1}{\sigma_k^2}[N(t_k) - N_c(t_k)]^2 = \sum_{k=1}^{n} \frac{[N(t_k) - N_c(t_k)]^2}{N(t_k)}$$
$$\chi_R^2 = \frac{\chi^2}{n-p} = \frac{\chi^2}{\nu} \quad (1)$$

where, $N(t_k)$ is the data point, $N_c(t_k)$ is the calculated value from the fit, n is the number of data points, p is the number of floating parameters, and $\nu=(n-p)$ is the number of degrees of freedom [12]. The value of χ_R^2 is expected to be near unity [12]. The best fits were obtained with one or two exponential fluorescence decay models with single chemical species for all the sunscreen samples in solvent and two species for sphere adsorbed sunscreen samples. However, a fixed-lifetime, variable-amplitude exponential (second or third exponential) of lifetime <40 ps was included in the fit. The quality of the fit is insensitive to variation of this lifetime from 40 ps to 0.01 ps ("zero" lifetime limit of the fitting program) and significantly reduced the χ_R^2 value for the padimate and cinnamate data. When this zero-lifetime component did not significantly improve the fit (reduce the value of χ_R^2), the amplitude of the component was zero or small. This state was introduced to account for any fast-relaxing state or residual scattering from the sample. Analysis of padimate O and octyl methoxy cinnamate data show that this additional exponential results in a fast radiative rate closer to the calculated value from the Strickler-Berg relation [13].

Emission filters Emissions from octyl salicylate and padimate O samples were filtered by 460 and 370 nm interference filters respectively. The interference filters have a bandwidth of 10 nm. Because of the weak fluorescence of octyl methoxy cinnamate, we used glass (absorbing) band pass filters BG-12 and KG-5 (Schott Glaswerke, Mainz, Germany) instead of an interference filter. Emission spectra of sunscreens and nanospheres are shown together with filter transmission spectra (Figs. 1, 2 and 3).

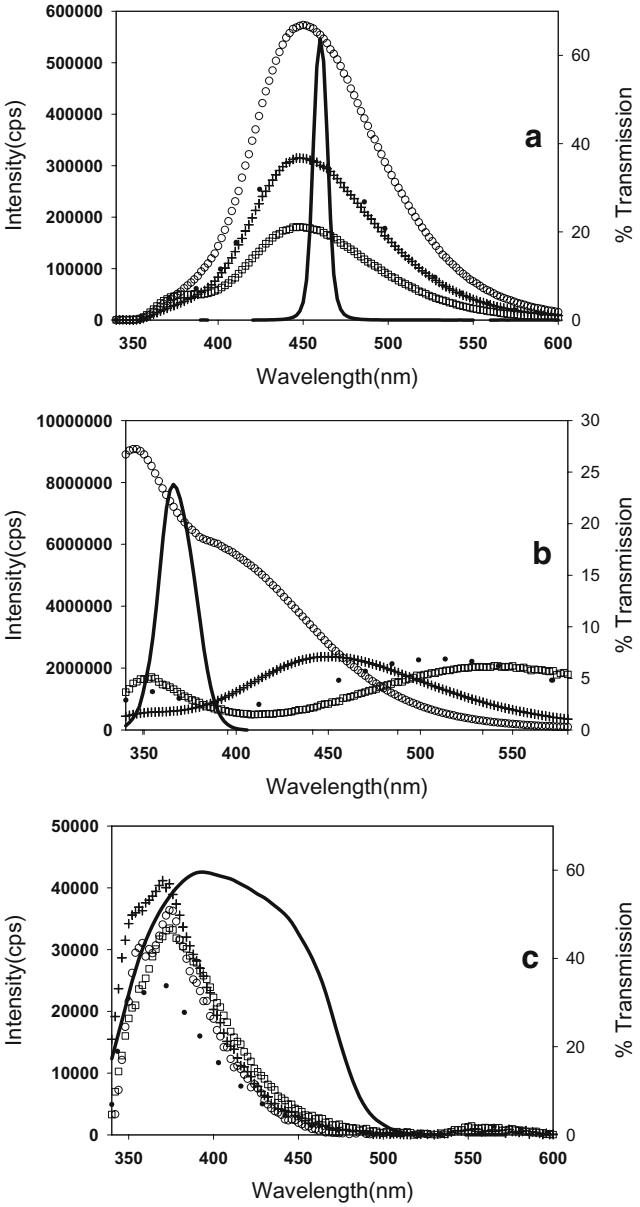

Fig. 1 Emission of sunscreens and filter transmission. Fluorescence of sunscreens **a** Octyl salicylate, **b** padimate O and **c** Octyl methoxy cinnamate in methanol (*empty square*), 1-propanol (*bullet*), ethyl-acetate (*plus sign*) and toluene (*empty circle*). Samples were excited at 310 nm. Filter transmission spectrum (*thick line*) **a** 460 nm interference filter, **b** 370 nm interference filter and **c** Band pass BG-12 and KG-5 glass filters

Results

Lifetime of excited octyl salicylate

Octyl salicylate showed emission at 460 nm from a single state with a lifetime of a few hundred picoseconds. Fitting the decay data with a two-exponential model showed the pre-exponential values of one of the exponents to be about 0.99,

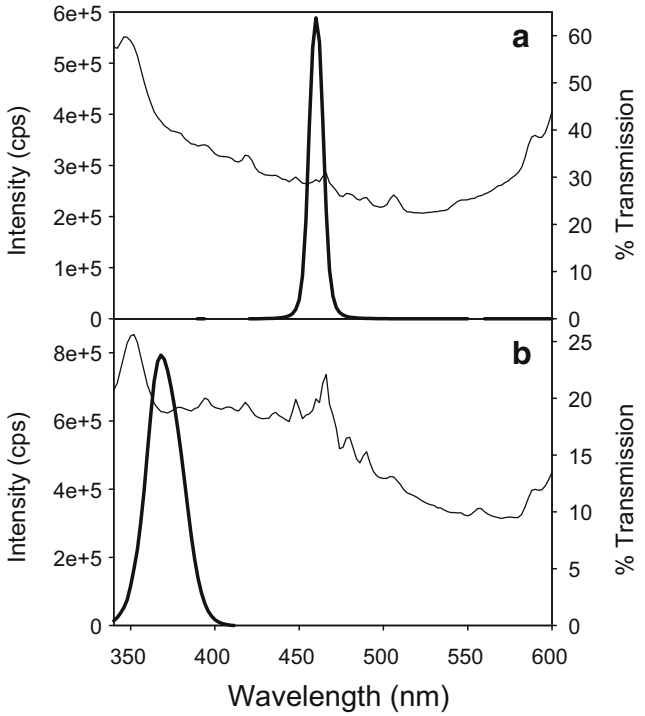

Fig. 2 Emission of 220 nm sphere and filter transmission. Fluorescence of 220 nm polystyrene spheres excited at 310 nm (*thin line*). Interference filters transmission spectrum (*thick line*) **a** 460 nm and **b** 370 nm. The emission fine structure is caused by whispering-gallery modes, not noise

which suggests that the decay of octyl salicylate is single exponential. The lifetime of octyl salicylate increased from 140 to 460 ps (Table 1), generally in order of decreasing solvent dielectric constant. (Salicylate in 1-propanol ($\varepsilon \approx 20$) and ethyl acetate ($\varepsilon \approx 6$) have almost equal lifetimes.). This increase in lifetime is obvious from the slope of the fluorescence decay curves between 1 and 3 ns in Fig. 4. The increase in lifetime was consistent with the observed increase in the steady-state emission intensity: the ratio of octyl salicylate's lifetime in a solvent to lifetime in methanol is close to the corresponding ratio of steady state fluorescence intensities [9]. Introduction of a fast relaxing state with lifetime 0.01 ps ("zero" lifetime) as a second exponential to the fit did not change the fit or its χ_R^2 value in most solvents. However, the decay of octyl salicylate in toluene showed a small contribution with pre-exponential value 0.03 (Table 1). Because no variation in the χ_R^2 value (1.05) for the fits with or without the fast-relaxing component, the contribution can be attributed to a small amount of scattering or slight shift in instrumental timing.

Lifetime of excited padimate O

Steady-state fluorescence of padimate O showed two emission peaks [9, 10] similar to the spectra observed for other dimethylamino molecules like *p*-(*N*,*N*-dimethylamino)benzoate, *p*-(*N*,*N*-dimethylamino)benzoic acid and *p*-(*N*,*N*-dimethylamino)benzonitrile [14–20]. The two peaks have been attributed to two different states, a locally-excited (LE) state (short wavelength) and a twisted intramolecular charge transfer (TICT) state (long wavelength). Being a (dimethylamino)benzoate, padimate O also shows dual emission [9, 10]. We therefore propose a TICT state in padimate O that may be forming by the twisting of dimethylamino group about the amino-phenyl bond (Fig. 5). The twisting can facilitate the displacement of electronic charge by bringing the lone pair of electrons in the nitrogen of dimethylamino group into the plane of the benzene ring (from being perpendicular to the plane of benzene ring), resulting in the TICT state. The twisting of the amino-phenyl bond is affected by changes in polarity of the medium. This effect of polarity was observed in steady-state fluorescence in the form of spectral shifts (long wavelength peak) and spectral shape changes. Fluorescence decay of padimate O measured with a 370 nm interference filter (Fig. 1) allowed contributions from both LE and TICT emissions, except for padimate O in methanol, in which TICT emission was at about 520 nm. We therefore fitted the padimate O data with a two-exponential model. Both lifetimes increased with decrease in dielectric constant (Table 1). The general lifetime increase is

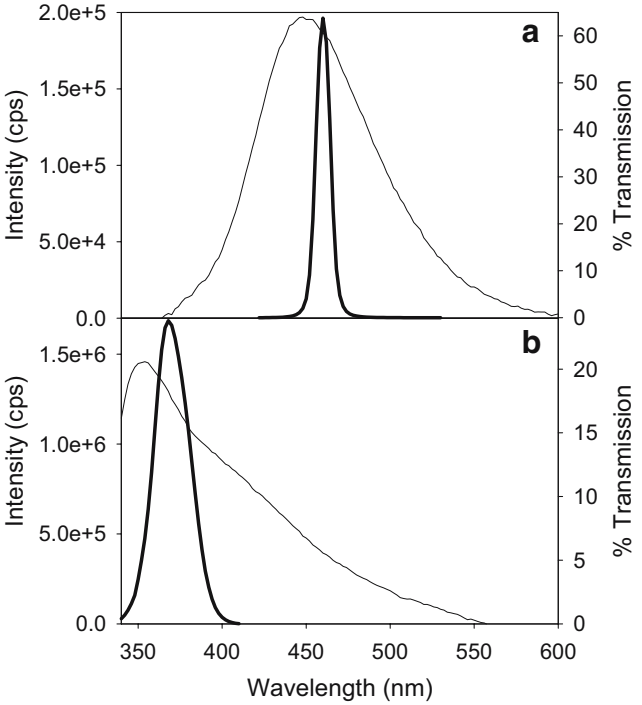

Fig. 3 Emission of sunscreens adsorbed to nanosphere and filter transmission. Fluorescence of sunscreens (*thin line*) adsorbed to 220 nm spheres **a** octyl salicylate and **b** padimate O. Samples were excited at 310 nm. Interference filters transmission spectrum (*thick line*) **a** 460 nm and **b** 370 nm

Table 1 Lifetime parameters of studied UV-B sunscreens in various solvents

	Zero lifetime state (See text.)		Sunscreen emission						
Solvent	τ_0 (ns)	α_0 (norm.) (±0.01)	τ_1 (ns) (±5%)	α_1 (norm.) (±0.01)	τ_2 (ns) (±5%)	a_2* (norm.) (±0.01)	χ^2	$\Sigma\tau_i\alpha_i$	Q ($\times10^{-2}$)
	Octyl salicylate								
MeOH	1×10^{-5}	0	0.14	0.99	–	–	1.32	0.15	0.6
1-Propanol	1×10^{-5}	0	0.25	0.99	–	–	1.09	0.27	1.1
Eth-ac	1×10^{-5}	0	0.24	0.99	–	–	1.19	0.24	1.0
Toluene	1×10^{-5}	0.03	0.46	0.97	–	–	1.05	0.49	1.9
	Padimate O								
MeOH	1×10^{-5}	0.78	0.19	0.22	–	–	1.50	0.04	0.07
1-Propanol	1×10^{-5}	0.75	0.21	0.04	0.65	0.21	1.21	0.14	0.4
Eth-ac	1×10^{-5}	0.79	1.44	0.09	3.68	0.12	1.21	0.56	3.8
Toluene	1×10^{-5}	0.38	1.61	0.06	3.36	0.56	1.15	1.98	9.8
	Octyl methoxy cinnamate								
MeOH	1×10^{-5}	0.96	0.36	0.04	–	–	1.07	0.02	0.08
1-Propanol	1×10^{-5}	0.94	0.39	0.05	–	–	1.35	0.04	0.07
Eth-ac	1×10^{-5}	0.96	0.54	0.04	–	–	1.14	0.03	0.1
Toluene	1×10^{-5}	0.93	0.86	0.06	–	–	1.37	0.12	0.09

Error intervals are averages. Actual intervals vary for each fit.
* Some "–" entries indicate values near zero that affect $\Sigma\tau_i\alpha_i$ and Q only slightly

clear from Fig. 6, in which the negative slope between 1 to 5 ns and 5 to 14 ns decreases from (a) to (d). Introduction of a short-lifetime exponential with lifetime between 1 and 0.01 ps to the fit did not change the other two exponential lifetimes but produced significant changes in ${\chi_R}^2$ values and residuals. Thus the three-exponential model appears to offer a better representation of padimate O decay. Repeating the decay measurements with long pass filters (GG385 and KG5, together transmitting from 370 to 780 nm, including the entire padimate O emission) instead of an interference filter (result not shown) showed no difference other than an increase in intensity (counts per sec). We believe these proposed LE and TICT states, modeled after those in structurally-related molecules that have been studied in more detail and with other methods [6], are reasonable for padimate O as well as for cinnamate (below), but additional evidence is desirable.

Lifetime of excited octyl methoxy cinnamate

It was difficult to observe fluorescence from octyl methoxy cinnamate with an interference filter because of cinnamate's weak emission. Hence we used band pass filters BG-12 and KG-5 to observe fluorescence decay (Fig. 1). While fitting the decays (Fig. 7) with different models, the best fits were obtained with a two-exponential model. In two-exponential fits the major contribution (pre-exponential amplitude) to the decays came from the short-lifetime exponent, about 90%. Variation of the short lifetime between 40 and 0.01 ps did not affect the fit or ${\chi_R}^2$ value but produced an anomalously large non-radiative rate, of the order of 10^{12} to 10^{14} s^{-1}, 10^4 times faster than the corresponding radiative rate. Hence we concluded that this short lifetime does not have a true radiative character and that the observed steady-state emission arises from the other component in the fit, the long lifetime exponent, for which the lifetime varied between 360 to 890 ps in different solvents. The pre-exponential (amplitude) contribution to the fluorescence decay from this exponential is less than 10%.

Strickler-Berg radiative rate

The radiative rate of the sunscreen can be calculated using the Strickler-Berg relation [12, 13]:

$$k_r = 2.88 \times 10^{-9} n^2 \frac{1}{\langle \lambda_{\mathrm{em}}^3 \rangle} \int \lambda \varepsilon(\lambda) \mathrm{d}\lambda \qquad (2)$$

where n is the refractive index of the medium, $<\lambda_{em}>$ is average emission wavelength, $\varepsilon(\lambda)$ is extinction coefficient of the sunscreen at wavelength λ and units of ε and λ are M^{-1} cm^{-1} and cm, respectively. The Strickler-Berg radiative rate for salicylate was close to the radiative rate computed as the ratio of quantum yield to lifetime of octyl salicylate (Table 3) because the emission was simple and came from a single state. For padimate O and octyl methoxy cinnamate the Strickler-Berg radiative rate was larger than the yield-determined radiative rate by a factor of 10–100 when the average lifetime (average of two exponentials) was used to

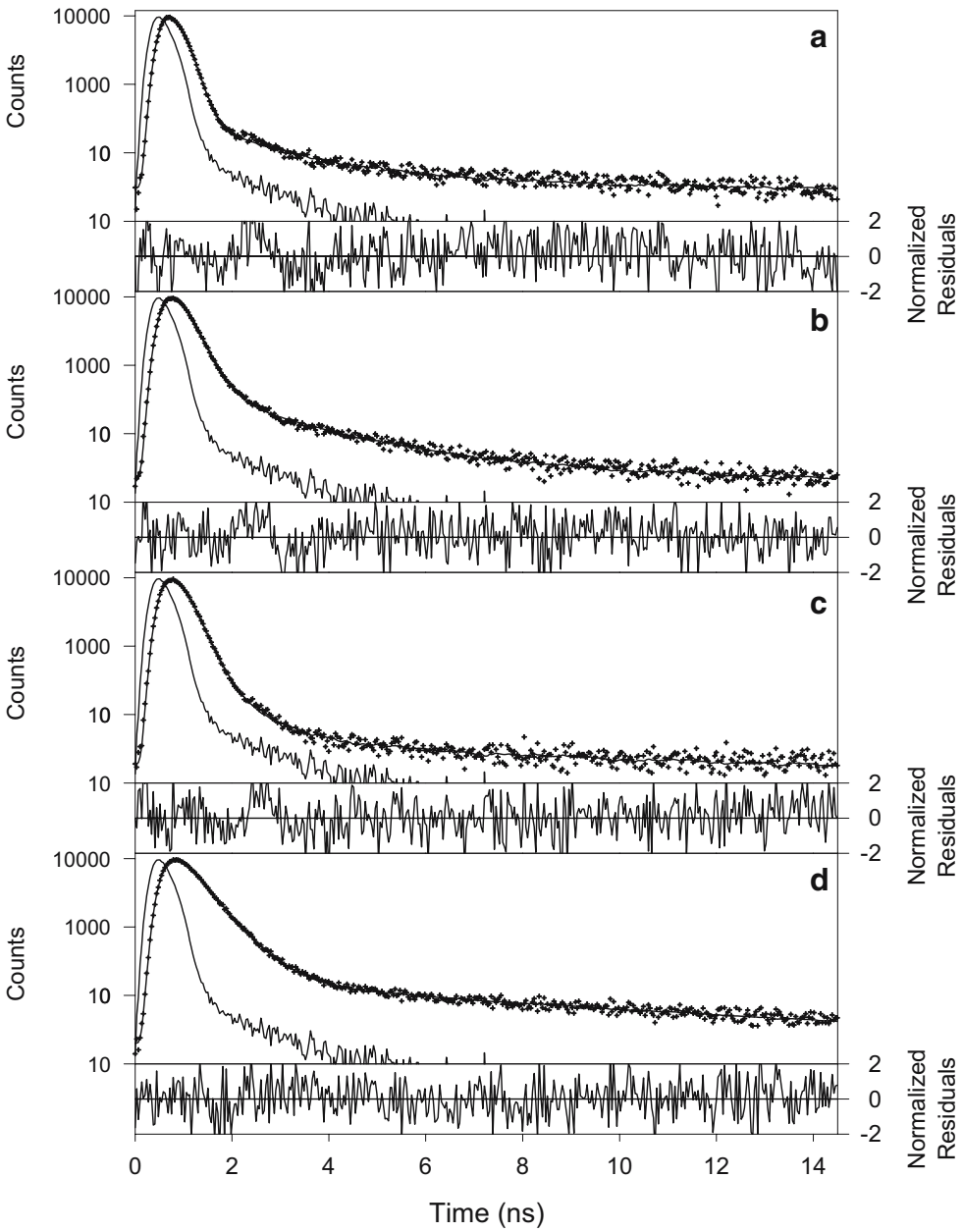

Fig. 4 Decay of octyl salicylate. Fluorescence decays of octyl salicylate in **a** Methanol, **b** 1-propanol, **c** Ethyl-acetate and **d** Toluene. Data (*series of plus signs*); Fits (*solid line*) and instrument response function (*solid line*). Weighted residuals at the bottom of each figure corresponding to the fit

obtain the calculated radiative rate (details in the calculated radiative rate section). However, the radiative rate calculated from the quantum yield of octyl methoxy cinnamate was between the upper and lower limit of the radiative rate computed from the short lifetime exponential alone. This result suggests the presence of two excited states in octyl methoxy cinnamate, a fast-relaxing state and a slow relaxing state. We term this second state a "dark state" in the discussion because of its lower radiative rate (though, surprisingly it is primarily responsible for the observed steady-state emission). Padimate O also produced a similar result when the radiative rate was computed using the short lifetime of the three exponential fit, indicating padimate O also has two excited states, a fast relaxing state, and a slow relaxing state.

Quantum yield of sunscreens

Since the quantum yields (Q) of the sunscreens were not available in the open literature we calculated them using the relation for quantum yield [12] given below,

$$Q = Q_R \frac{I}{I_R} \frac{OD_R}{OD} \frac{n^2}{n_R^2} \tag{3}$$

where I is the steady-state intensity integrated over emission wavelength, OD is the optical density and n is the refractive index. The subscript R refers to the reference fluorophore. For our quantum yield calculations we used the value 0.66 for Q_R, which is the quantum yield of the

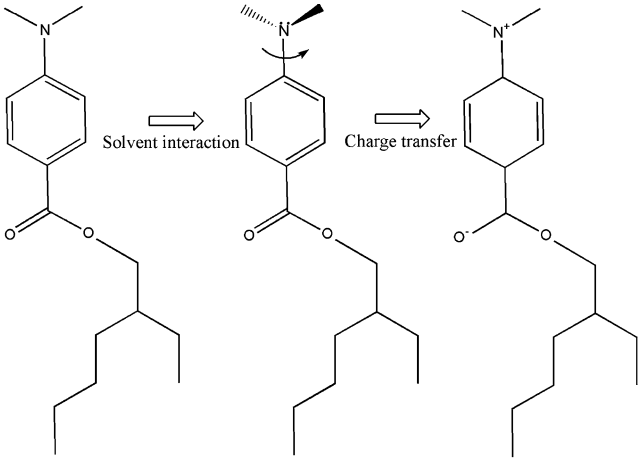

Fig. 5 Structural representation of padimate O's solvent interaction and intramolecular charge transfer

reference 2-aminopurine [21], which is excited and emits in the same region as the sunscreens. Except for octyl methoxy cinnamate the quantum yields (Table 3) increase with decrease in dielectric constant. The quantum yield can also be obtained by using integrated intensity from the time-resolved data. Hence the quantum yield $Q(\alpha, \tau)$ is also given by

$$Q(\alpha,\tau) = Q_R \frac{\left(K \sum_i \alpha_i \tau_i\right)}{I_R} \frac{n^2}{n_R^2} \frac{OD_R}{OD} \tag{4}$$

where, the integrated intensity I of the steady-state quantum yield is replaced by the sum of $\alpha_i\tau_i$ (α_is contain the radiative rates and numbers of molecules), I_R is the steady-state emission intensity of 2-aminopurine, and K is a constant which depends on steady-state and time-resolved instrumental and filter differences, hence calculated by equating steady-state Q with $Q(\alpha, \tau)$. Equation 3 assumes α_is and τ_is are independent of wavelength, which is what we observe (same padimate O results with interference and long pass filters). From the $Q(\alpha, \tau)$ relation the quantum yield of individual states were obtained.

Radiative rates

The ratio of a sunscreen's fluorescence quantum yield to corresponding lifetime provides the "measured" radiative rate (as opposed to "calculated" rate from the Strickler-Berg formula, with its associated spectra) of a particular excited state. The "measured" radiative rate of octyl salicylate in different solvents was nearly constant, about 4×10^7 s^{-1} (Table 3) and, as mentioned previously, is approximately equal to the calculated Strickler-Berg rate. The same "measured" radiative rate for octyl methoxy cinnamate for the emissive state obtained using average lifetime varied between 1×10^6 s^{-1} and 2×10^6 s^{-1} (Table 3), much less than the Strickler-Berg value. The small radiative rates were the reason for weak steady-state fluorescence.

The non-radiative rate showed unsystematic variation for both octyl salicylate and octyl methoxy cinnamate with dielectric constant (Table 3), suggesting an indirect relationship between the non-radiative rates and dielectric constant. In contrast to octyl salicylate and octyl methoxy cinnamate, the padimate O result was complex because the radiative rate varied strongly with dielectric constant. In addition to this variation with dielectric constant, radiative rates computed with the average lifetime obtained from two exponential fits were smaller by a factor of 10–100 than the Strickler-Berg radiative rate values. This led us to choose a three-exponential model to accommodate a fast relaxing state in padimate O. The short lifetime, together with quantum yield, leads to a "measured" radiative rate about equal to the Strickler-Berg value, while the average lifetime gives the much smaller radiative rate of the emissive state (termed the "dark state"). The complexity presented by padimate O to the analysis of fluorescence kinetics signifies the importance of a directly measured fluorescence lifetime of this molecule, in addition to the quantum yield and radiative rates.

Lifetime of excited octyl salicylate and padimate O adsorbed to 220 nm spheres

Analysis of polystyrene nanosphere emission alone showed two lifetimes, measured at 450 nm (Fig. 8c). We fit the decay of sunscreen (Fig. 8a,b) adsorbed to spheres with a two-species model. One species with two exponentials corresponds to the sphere emission, and the other species corresponds to the sunscreen, with one- and two-exponential decays for octyl salicylate and padimate emissions, respectively. Our approach to fitting sphere plus sunscreen data was two-phase, necessitated by the wavelength dependence of the lifetimes of the nanosphere emission and our desire to avoid attempts to perform four-exponential fits. In phase 1, for salicylate/sphere emission observed at 450 nm, we first fixed two lifetimes as those determined from samples of spheres alone and fit for a third lifetime, interpreted as that of salicylate. This was found to be close to the value observed for salicylate in toluene, confirming the similarity of toluene and nanosphere environments. In phase 2, we fixed one lifetime as that of salicylate in toluene and fit for two other lifetimes, interpreted as those of the spheres. These two lifetimes were close to those determined from sphere-alone samples, confirming the consistency of the fitting procedure. To obtain an optimal fit to salicylate/sphere data, we then allowed all three lifetimes to vary from these phase-2 values to minimize χ_R^2. These values are displayed in Table 2. For the padimate data recorded at 370 nm, we performed phase-2 fitting, initially fixing two lifetimes at values determined from padimate/toluene samples. Two additional

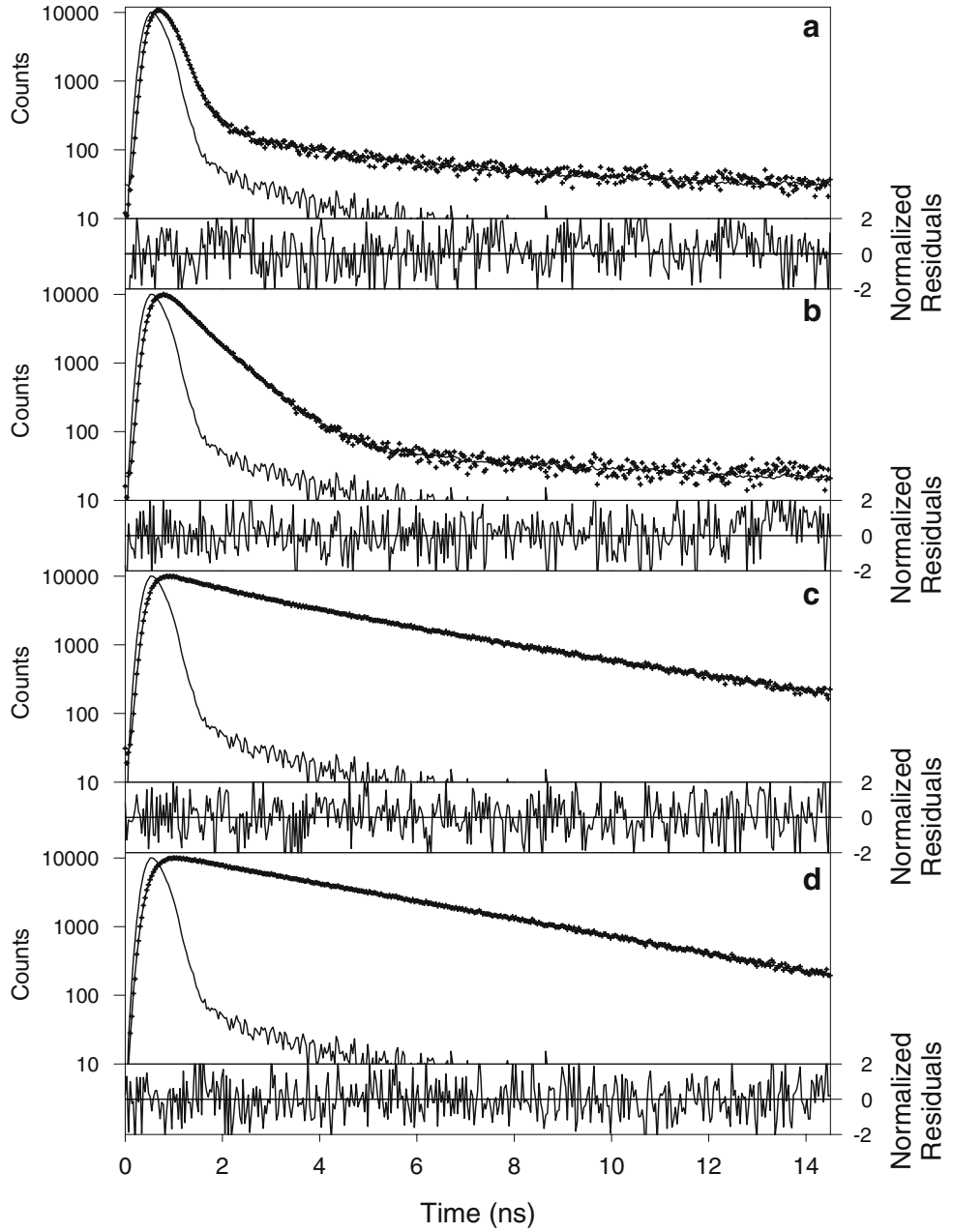

Fig. 6 Decay of Padimate O. Fluorescence decays of padimate O in **a** Methanol, **b** 1-propanol, **c** Ethyl-acetate and **d** Toluene. Data (*series of plus signs*); Fits (*solid line*) and instrument response function (*solid line*). Weighted residuals at the bottom of each figure corresponding to the fit

lifetimes were then fit, to get the two-exponentials corresponding to sphere emission at 370 nm. All four lifetimes were then allowed to vary (slightly) to obtain a best fit for all four lifetimes. In this fitting process, octyl salicylate adsorbed to 220 nm spheres (Fig. 8a) showed a lifetime of 620 ps for 450 nm emission while padimate O (Fig. 8b) showed 1.7 and 3.4 ns for the LE and TICT states emissions respectively (Table 2). These lifetime values were close to lifetimes observed for octyl salicylate and padimate O dissolved in low-polarity solvent toluene: 0.46, 1.61 and 3.36 ns, respectively. These lifetimes were consistent (discussed below) with the observed enhancement factor (previously defined relative to fluorescence with methanol as solvent) for salicylate and padimate O adsorbed to 220 nm sphere [9].

Enhancement factor

In steady-state experiments the fluorescence intensity enhancement factor of the sunscreen in the 220 nm sphere system was calculated from the ratio of fluorescence intensity

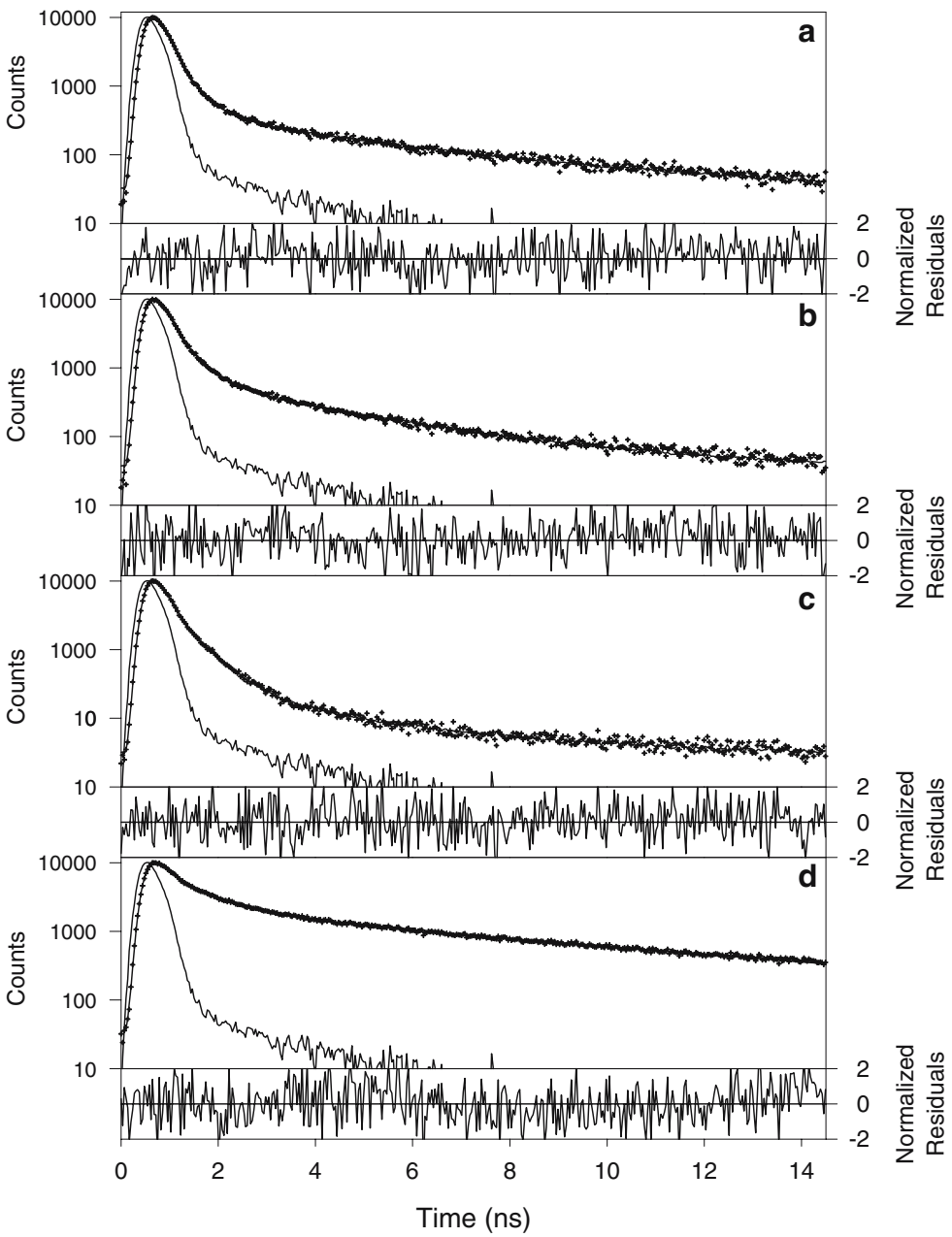

Fig. 7 Decay of octyl methoxy cinnamate. Fluorescence decays of octyl methoxy cinnamate in **a** Methanol, **b** 1-propanol, **c** Ethyl-acetate and **d** Toluene. Data (*series of plus signs*); Fits (*solid line*) and instrument response function (*solid line*). Weighted residuals at the bottom of each figure corresponding to the fit

at the peak wavelength (450 nm for salicylate and 360 nm for padimate O) of sunscreen adsorbed nanosphere to same sunscreen in methanol. The enhancement factors were 6.4 and 30 for octyl salicylate and padimate O respectively [9]. In time-resolved measurements, the ratio of lifetime (LE state for padimate O) when adsorbed to nanosphere to lifetime of sunscreen in methanol primarily determines the enhancement factor. The factors were 4.4 and 13 for octyl salicylate and padimate O, respectively, which are smaller than the values observed in steady-state results. However, the mere observation of enhancement in fluorescence lifetimes similar to the increase in lifetime of the sunscreens in toluene indicates that the molecules are present in low dielectric constant region in the mixed polarity, nanosphere environment.

Discussion

The primary objectives of this study were to elucidate (1) the excited-state processes occurring in three UV-B sunscreens following UV excitation, and (2) the solvent effect on the excited states and the implications for excited state processes. Secondarily, the fluorescence lifetimes of sunscreens in nanosphere suspension were used to test and substantiate the

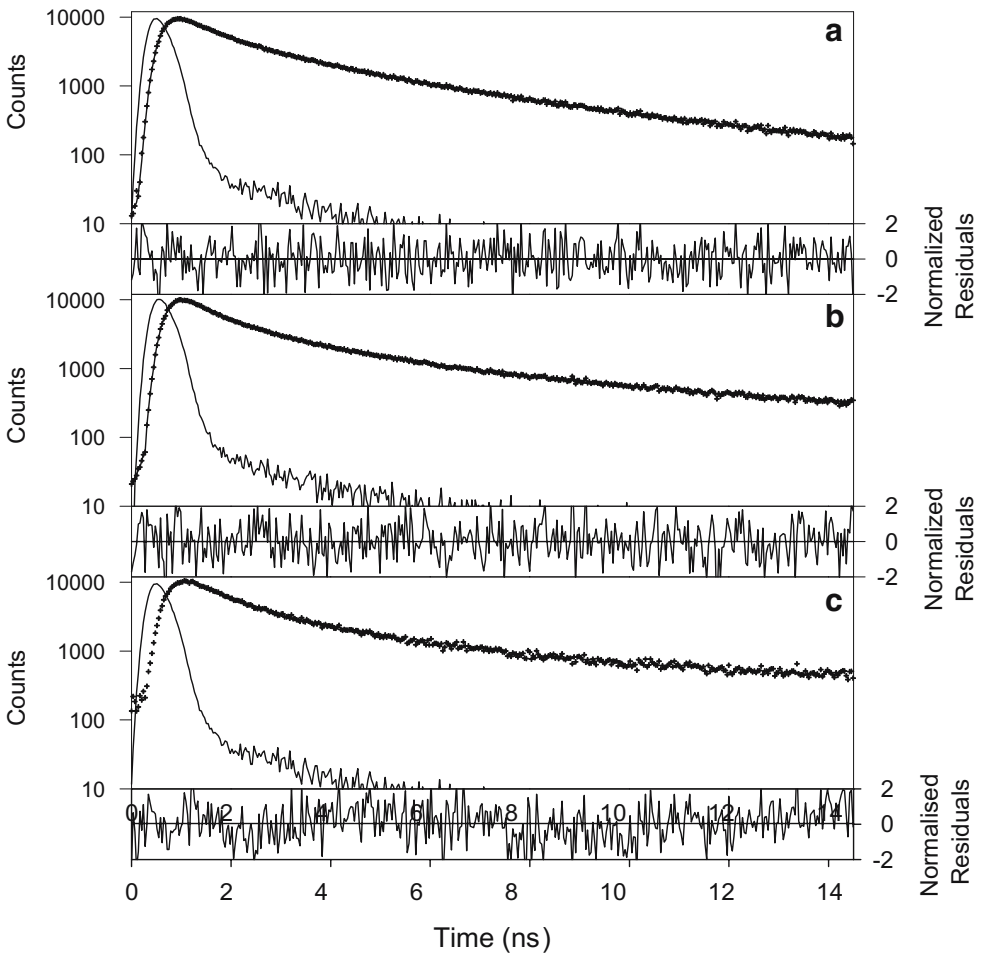

Fig. 8 Decay of sunscreen adsorbed to nanospheres**.** Fluorescence decays of octyl salicylate and padimate O adsorbed 220 nm spheres in **a** Octyl salicylate, **b** padimate O and **c** 220 nm sphere alone (without sunscreens). Data (*series of plus signs*); Fits (*solid line*) and instrument response function (*solid line*). Weighted residuals at the bottom of each figure corresponding to the fit

polystyrene nanosphere suspension as a model system for studying sunscreens in a mixed polarity environment.

In our previous work, we observed two emission peaks in steady-state fluorescence spectra of octyl salicylate in some solvents, the peak at 450 nm being the prominent one. In this work, we chose the prominent 450 nm emission because steady-state fluorescence of octyl salicylate adsorbed to polystyrene nanospheres (our suggested skin model system) [11], adsorbed to HaCat cells and applied to skin [10] showed 450 nm emission alone. The species of octyl salicylate emitting at 450 nm in the model system could be similar to the methyl salicylate species in cyclodextrin matrix [22], because the salicylate structure is the same as in methyl salicylate and the long chain (octyl) weakly interacts with photo-excited electrons. The explanation for methyl salicylate's 450 nm emission can therefore be used to explain the octyl salicylate excited state. The 450 nm emission must be from a species of octyl salicylate formed by hydrogen bonding between the –OH and the oxygen of the –C=O group of salicylate (Fig. 9), as observed in methyl salicylate [22–24].

The short lifetimes (Table 1) of the 450 nm emissions confirm that the large Stokes shift (about 150 nm from the

Table 2 Lifetime parameters of studied UV-B sunscreens adsorbed to 220 nm spheres

Sunscreens	In 220 nm sphere medium								
	Species 1: spheres				Species 2: sunscreen				
	τ_1 (ns)	α_1 (norm.)	τ_2 (ns)	α_2 (norm.)	τ_1 (ns)	α_1 (norm.)	τ_2 (ns)	α_2 (norm.)	χ^2
Octyl Salicylate (λ_{em}=460 nm)	2.03	0.41	5.97	0.32	0.62	0.27	–	–	1.02
Padimate O (λ_{em}=370 nm)	0.5	0.16	9.2	0.40	1.7	0.35	3.6	0.09	1.15

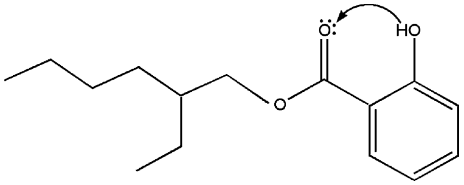

Fig. 9 Intramolecular hydrogen bonding of octyl salicylate (salicylate species emitting at 450 nm)

excitation wavelength) is not likely to be due to phosphorescence (triplet emission). Methyl salicylate and other salicylate ions also show this large Stokes shift and short lifetimes [22–25]. Change of solvent, that is, change of dielectric constant, did not change the steady-state emission spectral shape of octyl salicylate [9], but changed the quantum yield. This indicates that the low dielectric constant changes the kinetics without changing the energy level of the state. The radiative rate being constant for various solvents and comparable to the calculated radiative rate (Table 3) shows that the observed change in quantum yield with dielectric constant is due to a change in the non-radiative rate. The non-radiative rate decreases with decreasing polarity/dielectric constant of the medium, indicating there is a relationship between the non-radiative rate of octyl salicylate and solvent polarity/dielectric constant. The decrease is not continuous, as octyl salicylate in ethyl acetate (ε=6) and 1-propanol (ε=20) have the same non-radiative rate. The relationship between non-radiative rates and dielectric constants must be indirect. This is not surprising: a similar result is observed in methyl salicylate [23]. Hence, as suggested in reference [23] for methyl salicylate, the reason for the observed decrease in lifetime, quantum

Table 3 Photophysical parameters of sunscreens

Solvents	MeOH	1-Propanol	Eth-ac	Toluene
ε	32	20	6	2.4
Octyl salicylate				
λ_{abs} ±2 (nm)	306	306	306	308
Abs bandwidth ±2 (nm)	34	34	33	34
ε_a ($M^{-1}cm^{-1}$)	5,870	5,840	5,760	6,010
λ_{em} ±2 (nm)	450	450	450	452
$Q\times10^{-2}$	0.6	1.1	1.0	1.9
$<\tau>=(\Sigma\tau_i^2\alpha_i/\Sigma\tau_i\alpha_i)$ (ns)	0.15	0.27	0.24	0.46
$k_r\times10^7$ (s^{-1})	4.0	4.1	4.2	3.9
$k_{nr}\times10^9$ (s^{-1})	6.6	3.7	4.1	2.0
PadimateO				
λ_{abs} ±2 (nm)	309	310	306	309
Abs Bandwidth ±2 (nm)	52	52	51	52
ε_a ($M^{-1}cm^{-1}$)	38,300	38,300	37,700	39,000
	354	358	–	350
λ_{em} ±2 (nm)	515	495	446	410
$Q\times10^{-2}$	0.07	0.4	3.8	9.8
$<\tau>=\left(\sum\tau_i^2\alpha_i/\sum\tau_i\alpha_i\right)$ (ns)	0.2	0.6	3.2	3.3
$k_r\times10^6$ (s^{-1})	3.8	7.2	12	30
$k_{nr}\times10^9$ (s^{-1})	5.3	1.7	0.3	0.3
$k_r^*\times10^7$ (s^{-1})	21	21	18	33
$k_{nr}^*\times10^{13}$ (s^{-1})	1.3	1.2	0.9	2.2
Octyl methoxy cinnamate				
λ_{abs} ±2 (nm)	310	310	306	308
Abs Bandwidth ±2 (nm)	38	36	36	34
ε_a ($M^{-1}cm^{-1}$)	37,000	36,700	34,700	38,300
λ_{em} ±2 (nm)	385	380	380	380
$Q\times10^{-2}$	0.08	0.07	0.1	0.09
$<\tau>=\left(\sum\tau_i^2\alpha_i/\sum\tau_i\alpha_i\right)$ (ns)	0.4	0.4	0.5	0.9
$k_r\times10^6$ (s^{-1})	2.3	1.7	2.1	1.0
$k_{nr}\times10^9$ (s^{-1})	2.8	2.6	1.9	1.2
$k_r^*\times10^7$ (s^{-1})	39	51	41	44
$k_{nr}^*\times10^{12}$ (s^{-1})	1.0	1.0	1.0	1.2

* Calculated with k_r from Strickler-Berg formula. For salicylate the S-B rates are (only) 15–25% less than values determined from lifetime and quantum yield.

yield and increase in non-radiative rate of octyl salicylate in solvents of high dielectric constant could be due to an indirect effect of dielectric constant on intersystem crossing. The transition of excited octyl salicylate to the ground state is shown in the energy level diagram (Fig. 10) with a dielectric constant-dependent non-radiative rate. The lifetime of octyl salicylate adsorbed to 220 nm sphere is 620 ps, somewhat higher than the lifetime of octyl salicylate in toluene (460 ps). The enhancement factor of octyl salicylate from time-resolved measurement is somewhat smaller than the steady-state enhancement factor. Regardless of this small difference in the values, the fluorescence lifetime and enhancement result confirms the presence of octyl salicylate molecules in low dielectric region of nanosphere suspension.

Padimate O shows two emission peaks in steady-state, one of the peaks shifting to shorter wavelength with decrease in dielectric constant. The two peaks and their shifts make padimate O a complex molecule, in terms of calculating its quantum yield and understanding its emission kinetics. In this study we chose an interference filter (370 nm) which allowed contribution from both LE and TICT states.

Figure 11 shows the possible energy level diagram for padimate O's transition from excited to ground state. Because of the LE and TICT states in the emission we fit the fluorescence decay with a two-exponential model and used the average lifetime to compute the radiative rate of the emission. The radiative rates of padimate O in various solvent are of the order of 10^7 s^{-1}, values comparable to the radiative rates calculated using the method of Intermediate Neglect of Differential Overlap, with spectroscopic parameterization for dimethylamino molecules after including the intermolecular interactions (hydrogen bonding with solvents) [26–27]. However, they are smaller by a factor of 10–100 than the calculated radiative rate values using the Strickler-Berg relation. Further analysis of the decay data indicated the presence of a fast-relaxing state in addition to the slow-relaxing state. The energy level diagram shows the excited padimate O quickly relaxing into a dark state. The

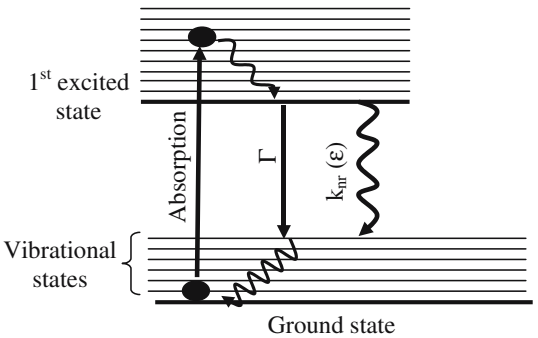

Fig. 10 Energy level diagram of octyl salicylate. Γ is the radiative rate and $k_{nr}(\varepsilon)$ is dielectric constant dependent non-radiative rate

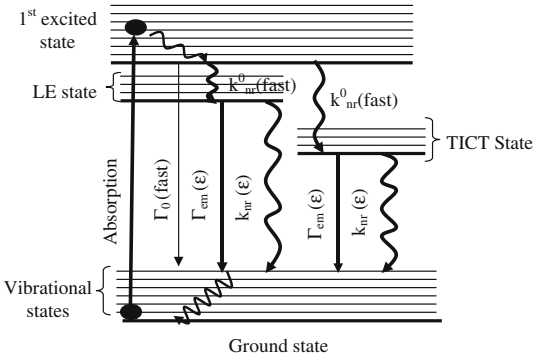

Fig. 11 Energy level diagram of padimate O with LE and TICT states. Γ_0 and k_{nr}^0 are the radiative rate and non-radiative rate of fast relaxation. $\Gamma_{em}(\varepsilon)$ and $k_{nr}(\varepsilon)$ are the dielectric constant dependent radiative and non-radiative rate of the emission

term "dark state" in this paper means a slow radiative rate; it is not completely dark. The steady-state emission is, in fact, primarily due to the transition from the dark to the ground state. There is little emission from the fast-relaxing state because the larger non-radiative rate (about 10^4 larger than radiative rate) makes the transition predominantly non-radiative. The fast-relaxing state may be the reason for the smaller quantum yield of padimate O than some common fluorophores, even though padimate O has larger extinction coefficient. After relaxing to the dark state the excited padimate O emits from either LE state or TICT state (smaller energy) with an average radiative rate $\Gamma(\varepsilon)$ (Fig. 11). The complexity, presence of a fast-relaxing state and emission from both LE and TICT states involved with excited state kinetics of padimate O, suggest that the lifetimes are critical physical parameters, in addition to the quantum yields and radiative rates. Thus, for padimate O the fluorescence lifetimes can be used as an indicator for polarity of the medium in which the molecule is present. Correcting for the overlapping emission from the polystyrene nanospheres near 360 nm and their two-exponential decay, the lifetime of LE-state padimate O adsorbed to nanospheres is found to be 1.7 ns, 13 times higher than the lifetime of the LE state of padimate O in methanol. The TICT state lifetime is 3.6 ns. These values are comparable to the lifetimes of padimate O in toluene, which indicates padimate O molecules prefer a low dielectric constant/low polarity environment when present in the heterogeneous medium of nanosphere suspension. Similar to our nanosphere suspension model system, α and β cyclodextrin matrices were considered as a heterogeneous model system to study the dimethlyamino molecule and methyl salicylate [17, 22]. References [17] and [22] showed the preference for low polarity matrix by dimethlyamino and salicylate molecules and the corresponding fluorescence enhancement. In our earlier studies, we showed such enhancement in octyl salicylate and padimate O when present in heterogeneous media formed by polystyrene

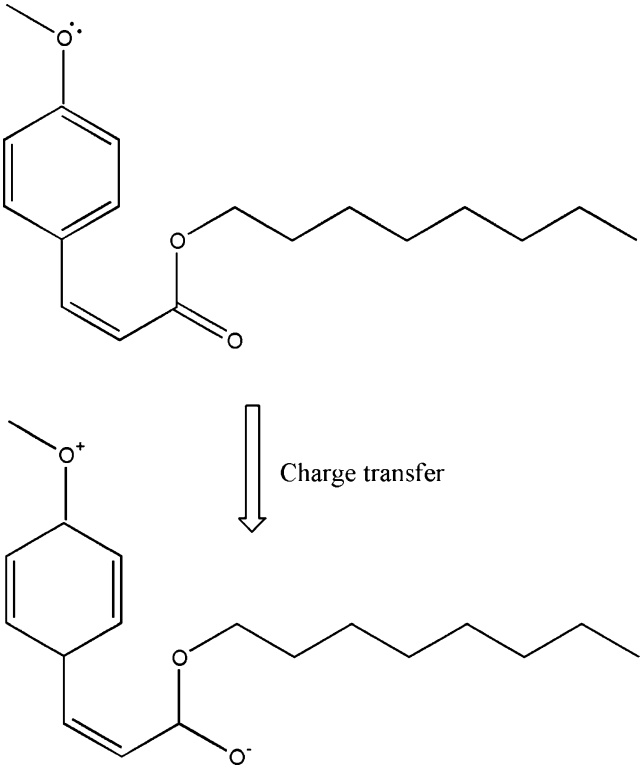

Fig. 12 Structural representation of octyl methoxy cinnamate's intramolecular charge transfer

nanospheres and skin cells. These lifetime results confirm the effects of polarity on the sunscreen molecules and shows that polystyrene nanospheres can be used as a model system superior to neat solvents for studying sunscreen. (Sunscreen applied to skin is in a heterogeneous system.)

Steady-state fluorescence intensities [9] and lifetimes of octyl methoxy cinnamate (Table 1) show weak dependence of fluorescence on change in dielectric constant of the medium. The small radiative-rate and large non-radiative values reiterate weak emission (Table 3). The large values for non-radiative rate indicate that there could be strong solvent interaction with octyl methoxy cinnamate, though not strong enough to shift the spectra. There is an electron lone pair in the methoxy oxygen, hence there could be charge transfer and a conformation change similar to those in padimate O (formation of LE and TICT states), but the steady-state spectra of octyl methoxy cinnamate did not show dual emission. Since the lone pair of electrons in oxygen is in the plane of benzene ring, cinnamate molecules need not twist to distribute the electronic charge and form the charge transferred state. Octyl methoxy cinnamate could be in its charge-transferred form (Fig. 12) most of the time and form hydrogen bonds with many solvents. Alternatively, the O–CH_3 group may be rapidly rotating, populating both (pre-) states in the ground state and/or in the excited state. (See discussion in next paragraph.) The Raman spectroscopic studies [6] showed octyl methoxy cinnamate's strong tendency to hydrogen bond with solvents when compared to padimate O. Reference [6] suggests that even a low polarity medium induces a structural change from benzonoid to quinoniod through charge transfer. These strong charge transfer and inter-molecular hydrogen bonding abilities cause the weak emission in cinnamate. Similar to padimate O, octyl methoxy cinnamate has two radiative rates: a fast rate for transition from excited to the dark state and a slow rate for transition from the dark state to ground state (Fig. 13). Again, we do not see the emission from the fast-relaxing state because the transition is mostly non-radiative ($k_r<0.001\ k_{nr}$). The transition from the dark state in octyl methoxy cinnamate is simpler than in padimate O because cinnamate emits from a single state. In addition to these results, weak fluorescence and short lifetimes confirm that the dielectric constant or the polarity does not significantly affect the emission of octyl methoxy cinnamate. Whatever the mechanism, the large non-radiative rates show that the excitation energy is efficiently dissipated through the non-radiative process. Thus, photophysically octyl methoxy cinnamate is superior to octyl salicylate and padimate O when used as a sunscreen because of its large absorption bandwidth, high extinction coefficient in the UV-B region and efficient conversion of absorbed energy, presumably to heat. Further, the independence of emission properties of octyl methoxy cinnamate on the polarity/dielectric constant of the medium indicates that the heterogeneity of skin may not have an effect on cinnamate's optical properties.

Our discussion of the structural and energy-state models for padimate O and cinnamate shown in Figs. 5, 11, 12 and 13 have left a key question unanswered: do the proposed LE and TICT structures exist only in the excited state or are they also present in the ground state? If both, are the relative populations similar in excited and ground states? The cited Raman data imply that in molecules analogous to padimate,

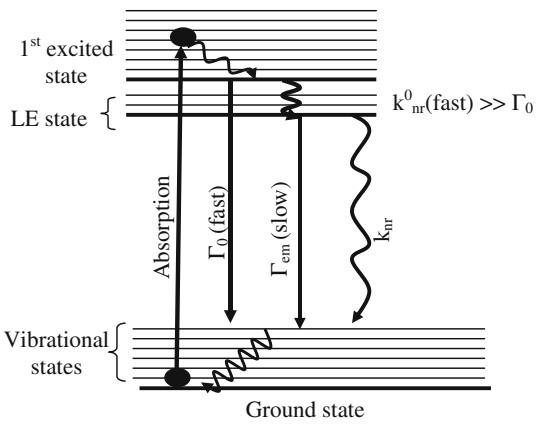

Fig. 13 Energy level diagram of octyl methoxy cinnamate. Γ_0 and k^0_{nr} are the radiative rate and non-radiative rate of fast relaxation. Γ_{em} and k_{nr} are the radiative and non-radiative rate of the emission

the rotated dimethylamino state and the charge-transferred state can exist before excitation. If all states were significantly populated in the ground state, the (pre-)LE, or and (pre-)TICT states would, however, be largely invisible to absorption spectroscopy, as low extinction coefficients (100× lower) presumably accompany the low radiative rates we have postulated and would be invisible in absorption spectra. (The absorption spectrum would be dominated by the structure to the left in Fig. 5.) Careful measurement of the fluorescence excitation spectrum in the long-wavelength (320–420-nm) region might provide evidence of these directly-excited states, but this is made more difficult by the presence of solvent Raman bands. If a large fraction of ground-state padimate O molecules existed in the states of low radiative rate, the extinction coefficient for the left-most, high radiative-rate padimate structure in Fig. 5 would have to be correspondingly higher than the already high value of 38,000 M^{-1} cm^{-1}. We presently prefer a model in which the LE and TICT states of padimate form in the excited state. A further question: are these states in equilibrium? Our data do not provide a definitive answer. Estimations of the needed thermally-activated back-reaction rates LE→E* and TICT→E* would demand a rather large, positive (favorable) ΔS of activation to overcome the required activation energy. However, the temperature dependence of the rates should be studied to clearly answer this question. For cinnamate, analogous structure vs. state questions must be addressed.

In summary, we have discussed the effect of solvent on the possible de-excitation pathways of three UV-B sunscreens and the preference shown by the sunscreens for the low dielectric environment in a heterogeneous medium. The analysis shows the de-excitation pathways of padimate O and octyl methoxy cinnamate are complex, with the presence of a fast-relaxing state and a dark state (causing weak emission). Although the complexity of padimate O is obvious from steady-state emission (two peaks), the results for cinnamate are surprising because the spectra and decays are simple. However, the large cinnamate extinction coefficient and contrasting weak fluorescence may be reflecting this complexity. Hence, the presence of two radiating states in padimate O and octyl methoxy cinnamate could be arising from their intra-molecular charge transfer and inter-molecular hydrogen bonding capabilities.

Acknowledgements Supported in part by a grants from NCI (CA94327) and from the University of Alabama at Birmingham (Preparing Future Faculty award and GAPF graduate fellowship, support of R. K.).

References

1. Azevedo JS, Viana NS Jr, Soares CD (1999) UVA/UVB sunscreen determination by second-order derivative ultraviolet spectrophotometry. Farmaco 54:573–578
2. Maier H, Schauberger G, Brunnhofer K, Honigsmann H (2001) Change of ultraviolet absorbance of sunscreens by exposure to solarsimulated radiation. J Investig Dermatol 117:256–262
3. Rosenstein BS, Weinstock MA, Habib R (1999) Transmittance spectra and theoretical sun protection factors for a series of sunscreen-containing sun care products. Photodermatol Photoimmunol Photomed 15:75–80
4. Serpone N, Salinaro A, Emeline AV, Horikoshi S, Hidaka H, Zhao J (2002) An in vitro systematic spectroscopic examination of the photostabilities of a random set of commercial sunscreen lotions and their chemical UVB/UVA active agents. Photochem Photobiol Sci 1:970–981
5. Lowe NJ (1997) Sunscreens: development, evaluation, and regulatory aspects, cosmetic science and technology series, 2nd edn. Marcel Dekker, New York
6. Beyere L, Yarasi S, Loppnow GR (2003) Solvent effects on sunscreen active ingredients using Raman spectroscopy. J Raman Spectrosc 34:743–750
7. Schlumpf M, Cotton B, Conscience M, Haller V, Steinmann B, Lichtensteiger W (2001) In vitro and in vivo estrogenicity of uv screens. Environ Health Perspect 109:239–244
8. Gupta VK, Zatz JL, Rerek M (1999) Percutaneous absorption of sunscreens through micro-yucatan pig skin in vitro. Pharm Res 16:1602–1607
9. Krishnan R, Carr A, Blair E, Nordlund TM (2004) Optical spectroscopy of hydrophobic sunscreen molecules adsorbed to dielectric nanospheres. Photochem Photobiol 79:531–539
10. Krishnan R, Pradhan S, Timares L, Katiyar SK, Elmets CA, Nordlund TM (2006) Fluorescence of sunscreens adsorbed to dielectric nanospheres: parallels to optical behavior on HaCat cells and skin. Photochem Photobiol 82:1557–1565
11. Krishnan R, Elmets CA, Nordlund TM (2006) New method to test the effectiveness of sunscreen ingredients in a novel nano-surface skin cell mimic. Photochem Photobiol 82:1549–1556
12. Lakowicz JR (1999) Principles of fluorescence spectroscopy, 2nd edn. Plenum, New York
13. Strickler SJ, Berg RA (1962) Relationship between absorption intensity and fluorescence lifetime of molecules. J Chem Phys 37 (4):814–822
14. Zhang CH, Chen ZB, Jiang YB (2004) Intramolecular charge transfer dual fluorescence of p-dimethylaminobenzoates. Spectrochimica Acta A 60:2729–2732
15. Sun YP, Bowen TL, Bunker CE (1994) Formation and decay of the ethyl *p*-(*N*,*N*-dimethylamino)benzoate twisted intramolecular charge transfer stated in the vapor phase, supercritical fluids and room temperature solutions. J Phys Chem 98:12486–12494
16. Kim YH, Cho DW, Yoon M (1996) Observation of hydrogen bonding effects on twisted intramolecular charge transfer of *p*-(*N*, *N*-dimethylamino)benzoic acid in aqueous cyclodextrin solutions. J Phys Chem 100:15670–15676
17. Nag A, Dutta R, Chattopadhyay N, Bhattacharyya K (1989) Effect of cyclodextrine cavity size on twisted intramolecular charge transfer emission: dimethylamino benzonitrile in β-cyclodextrine. Chem Phys Lett 157:83–86
18. Soujanya T, Saroja G, Samata A (1995) AM1 study of the twisted intramolecular charge transfer phenomenon in *p*-(*N*, *N*-dimethylamino)benzonitrile. Chem Phys Lett 236:503–509
19. Hicks JM, Vandersall MT, Babarogic Z, Eisenthal KB (1985) The dynamics of barrier crossings in solution: the effect of solvent polarity dependent barrier. Chem Phys Lett 116:18–24
20. Wang Y, Eisenthal KB (1982) Picosecond dynamics of twisted internal charge transfer phenomena. The role of solvent. J Chem Phys 77:6076–6082
21. Jean JM, Hall KB (2000) Theoretical studies of excited state properties and transitions of 2-aminopurine in the gas phase and in solution. J Phys Chem A 104:1930–1937

22. Cox GS, Turro NJ (1984) Methyl salicylate fluorescence as a probe of the geometry of complexation to cyclodextrins. Photochem Photobiol 40:185–188
23. Smith KK, Kaufmann KJ (1981) Solvent dependence of the non-radiative decay rate of methyl salicylate. J Phys Chem 85:2895–2897
24. Smith KK, Kaufmann KJ (1978) Picosecond studies of intramolecular proton transfer. J Phys Chem 82:2286–2291
25. Friedrich DM, Wang Z, Joly AG, Peterson KA, Callis PR (1999) Ground-state proton-transfer tautomer of the salicylate anion. J Phys Chem A 103:9644–9653
26. Artyukhov VYa, Smirnov OV (2003) Investigation of dual fluorescence in 4-dimethylamino benzonitrile. Rus Phys J 46:484–487
27. Artyukhov VYa, Smirnov OV (2004) Dual fluorescence in donor-acceptor molecules and the effect of fluorination. Rus Phys J 47:983–987